Article

Spatial and Temporal Variability of Ice Algal Trophic Markers—With Recommendations about Their Application

Eva Leu [1],*, **Thomas A. Brown** [2], **Martin Graeve** [3], **Jozef Wiktor** [4], **Clara J. M. Hoppe** [3], **Melissa Chierici** [5,6], **Agneta Fransson** [6,7], **Sander Verbiest** [8,9], **Ane C. Kvernvik** [8] and **Michael J. Greenacre** [1,10]

1   Akvaplan-Niva, CIENS, Gaustadalléen 21, 0349 Oslo, Norway; michael.greenacre@gmail.com
2   Scottish Association of Marine Sciences, Oban PA37 1QA, UK; t2001b@hotmail.com
3   Alfred-Wegener-Institute, Helmholtz-Centre for Polar and Marine Research, 27570 Bremerhaven, Germany; martin.graeve@awi.de (M.G.); clara.hoppe@awi.de (C.J.M.H.)
4   Institute of Oceanology Polish Academy of Science, 81-712 Sopot, Poland; wiktor@iopan.gda.pl
5   Institute of Marine Research, Fram Centre, 9007 Tromsø, Norway; melissa.chierici@hi.no
6   Department of Arctic Geophysics, University Centre of Svalbard, 9171 Longyearbyen, Svalbard, Norway; agneta.fransson@npolar.no
7   Norwegian Polar Institute, 9296 Tromsø, Norway
8   Department of Arctic Biology, University Centre of Svalbard, 9171 Longyearbyen, Svalbard, Norway; sanderverbiest@gmail.com (S.V.); AneK@unis.no (A.C.K.)
9   Department of Earth Sciences, Utrecht University, Heidelberglaan 8, 3584 Utrecht, The Netherlands
10 Department of Economics and Business, Universitat Pompeu Fabra, 08002 Barcelona, Spain
*   Correspondence: eva.leu@akvaplan.niva.no

check for updates

Abstract: Assessing the relative importance of sea ice algal-based production is often vital for studies about climate change impacts on Arctic marine ecosystems. Several types of lipid biomarkers and stable isotope ratios are widely used for tracing sea ic-associated (sympagic) vs. pelagic particulate organic matter (POM) in marine food webs. However, there has been limited understanding about the plasticity of these compounds in space and time, which constrains the robustness of some of those approaches. Furthermore, some of the markers are compromised by not being unambiguously specific for sea ice algae, whereas others might only be produced by a small sub-group of species. We analyzed fatty acids, highly branched isoprenoids (HBIs), stable isotope ratios of particulate organic carbon (POC) ($\delta^{13}C$), as well as $\delta^{13}C$ of selected fatty acid markers during an Arctic sea ice algal bloom, focusing on spatial and temporal variability. We found remarkable differences between these approaches and show that inferences about bloom characteristics might even be contradictory between markers. The impact of environmental factors as causes of this considerable variability is highlighted and explained. We emphasize that awareness and, in some cases, caution is required when using lipid and stable isotope markers as tracers in food web studies and offer recommendations for the proper application of these valuable approaches.

Keywords: trophic marker; lipid; fatty acid; highly branched isoprenoid (HBI); IP_{25}; H-Print; stable isotope ratio; compound-specific isotope analysis

1. Introduction

In a rapidly warming Arctic, primary production regimes are expected to change, and probably shift towards a larger contribution of phytoplankton, relative to sea ice algae, in response to increasingly

open waters and thinning sea ice [1]. These changes are likely to have far-reaching implications for the entire marine ecosystem, although they often remain difficult to assess or predict in detail. In the Bering Sea, a regime shift from a primarily benthic to a more pelagic food web has been observed over the past two decades and was attributed to decreased ice algal production [2,3]. The relevance of sea ice algal production for different parts of the polar ecosystem, ranging from key pelagic grazers to mammals has been studied extensively [4–7]. Another important aspect addressed in various studies has been assessing the overall strength of sympagic-pelagic or sympagic-benthic coupling [8–10]. Despite using different approaches, the key interest in all these studies is quantifying the relative importance of biomass produced by sea ice algae (as opposed to phytoplankton) for higher trophic level production. Different types of trophic markers are widely applied to analyze food web structure, based on numerous assumptions of how sea ice algae differ biochemically from phytoplankton. Here we will focus on two common types of trophic markers: (a) lipid-based trophic markers (fatty acid trophic markers, and highly branched isoprenoids), and (b) $\delta^{13}C$ as one example of a stable isotope-based marker technique.

1.1. Fatty Acid Trophic Markers (FATM)

The repertoire of fatty acids in an algal cell is determined genetically and differs between major algal groups (for a recent review, see [11]). These fatty acids are taken up as part of a consumer's diet, and partly incorporated unchanged into the lipids of animals at higher trophic levels. Hence, fatty acids can be used to trace the type of algae that an organism has been feeding on [12]. This concept works best for essential polyunsaturated fatty acids (PUFAs) that are synthesized de novo exclusively by algae in the marine food web, since other fatty acids found in higher organisms might be of non-algal origin. Furthermore, it has been shown that the relative abundances of fatty acids in algae may vary considerably depending on the environmental conditions, such as light, nutrient concentrations, and temperature [13–18]. Applying FATM to distinguish specifically between sea ice algae and phytoplankton as the source of lipids, however, is hampered by the fact that this distinction relies on the taxonomic composition of these two blooms being sufficiently distinct to be reflected in clearly different fatty acid profiles. However, quite frequently diatoms account for the dominating part of the biomass in both pelagic and sympagic spring blooms.

1.2. Highly Branched Isoprenoids (HBIs)

Produced only by diatoms, HBIs are alkene biomarkers that have been used increasingly as specific indicators for sea ice algae, both in food web studies, but also as paleo-proxies for studying the position of the sea ice edge in the past [19,20]. Some HBIs are produced specifically by a number of Arctic pennate diatoms including species within the genera of *Haslea, Pleurosigma,* and *Rhizosolenia* [19,21]. A monounsaturated HBI with 25 carbon atoms was identified as specific to a subset of Arctic sea ice diatoms [19,22] and termed the "Ice Proxy" or IP_{25} [20] IP_{25} is chemically stable and becomes incorporated unaltered into organisms at higher trophic levels and, due to its source specificity, is an excellent tracer for carbon fixated by sea ice algal primary production. The distribution of IP_{25} in sea ice broadly corresponds to the ice algal bloom peak, with the highest concentrations being measured nearer the ice-water interface and mostly in the lower 1–5 cm horizon of sea ice [23,24]. The diatom species producing this compound usually account for 1–5% of sea ice diatoms, while the most dominant species (e.g., *Nitzschia* spp.) are not producing it [19]. Alongside IP_{25}, a suite of HBI isomers have been identified as providing specific indicators for either pelagic or sympagic microalgae [25]. This enabled the development of an index for the relative proportion of sympagic to pelagic HBIs, the so-called H-Print [26]. Recently, the production rate of certain HBIs was found to increase strongly under nutrient limiting conditions in the sea ice diatom *Haslea vitrea*, indicating some sort of environmental control of the cellular content of these compounds [27].

1.3. Carbon Stable Isotope Ratios ($\delta^{13}C$)

A further trophic marker approach used to identify sea ice algae is based on the ratio between the two stable isotopes of carbon, ^{12}C and ^{13}C, expressed as $\delta^{13}C$ (‰). This ratio is widely applied in trophic food web analyses, but the basis for its specific use to contrast sea ice algae vs. phytoplankton is the relative shortage of inorganic carbon for photosynthesis in spatially limited brine channels where high biomass densities might accumulate, as opposed to a usually well replenished surface layer of the ocean. As a result, $\delta^{13}C$ values in sympagic algae become enriched over time by ^{13}C. A strong impact of both nutrient availability as well as taxonomic composition on sympagic particulate organic carbon (POC) $\delta^{13}C$ was described previously [28], and the implications for tracing the fate of ice algal production in Arctic food webs is discussed extensively both in this work, as well as more recently [29]. One caveat of this approach is that Arctic phytoplankton can also exhibit considerable base-line variation in its isotope values which can result in overlaps with sea ice algae, complicating food-web analyses [30].

In order to mitigate some of the shortcomings of the above described approaches, and to increase the specificity, it is possible to measure $\delta^{13}C$ values not only for total POC, but also for specific compounds, such as individual fatty acids (termed compound-specific isotope analysis, CSIA of fatty acids, FAs). This approach has been successfully applied to Arctic and Antarctic food webs [7]. For example, a combination of FATM and CSIA of FAs was used to describe and distinguish between ice-associated and pelagic particulate organic matter (i-POM vs. p-POM) in a study from the Bering Sea [31].

Allof these analytical methods and approaches have their specific advantages and shortcomings, which will be discussed in the later part of this article. Although large-scale food-web analyses understandably require some level of generalization, it is crucial to be aware that none of these markers in primary producers are constant. Rather, their occurrence and abundance depend strongly on both taxonomic composition and physiological status of the organism in question, which ultimately are controlled by environmental conditions and concurrent growth phase. For isotopic signatures in bottom sea ice POC and particulate organic nitrogen (PON), such interactions were described and discussed thoroughly previously [28].

There is some information available on the dynamics of some of these markers on both species, and even more importantly, community level; however, studies measuring all of them simultaneously are very rare. Spring bloom dynamics of primary producers in high latitudinal ecosystems are highly unpredictable and quite dynamic, and we therefore expect correspondingly high variability in the trophic marker signatures during pre-, peak- and post-bloom stages. The aim of our study was to document the spatial and temporal variability of different lipid and stable isotope-based trophic markers during an ice algal spring bloom and relate it to environmental conditions, as well as taxonomic composition. We then used these data to compare and contrast the reliability of each approach to distinguish between sympagic and pelagic POM.

2. Materials and Methods

All data were collected during spring/summer 2017 as part of the FAABulous project (Future Arctic Algae Blooms—and their role in the context of climate change) in Van Mijenfjorden in Svalbard (Norway).

2.1. Site Description

Located on the western coast of Spitsbergen, Van Mijenfjorden has maximum water depths ranging from ca. 70 m in the inner basin to ca. 100 m in the outer basin and is semi-closed by the Akseløya island (Figure 1), located close to its entrance. Together with a shallow sill, this island limits the inflow of Atlantic water such that stable ice cover can form within the fjord from December/January until June/early July [32]. Due to the strongly increased winter temperatures in Svalbard, however, ice formation has become more variable and weaker during the past 10–15 years, resulting in a shorter period of ice

coverage [33]. In 2017, sea ice started to form and stabilize around the end of January/early February in the innermost part of the fjord, but did not reach thicknesses (>0.2–0.3 m) that allowed safe working conditions before early March. A sea ice observatory was installed close to the deepest part of the inner basin on 8th of March providing background data for the entire study period on sea ice thickness, snow cover, and transmittance. Sea ice algal development was followed by sampling different stations in the inner basin from early March to early May 2017, including a spatial transect starting from a very shallow station close to the shore (IS) to the mid-fjord station VMF2 (Figure 1).
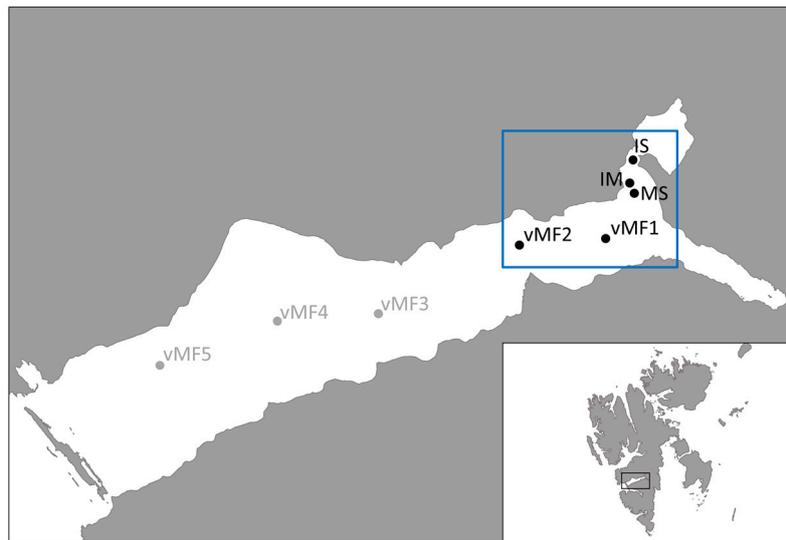
Figure 1. Sampling transect of the FAABulous project in Van Mijenfjorden, Svalbard. The sea ice samples were taken from the five innermost stations (IS, IM, MS, VMF1, VMF2) as sea ice coverage was rather poor and not covering the entire fjord in winter/spring 2016/2017.

2.2. Sampling

Sampling was conducted on landfast ice near the settlement of Svea, in Van Mijenfjorden, Spitsbergen from 3 March to 2 May 2017. Sea ice core samples (bottom 0–3 cm) were usually collected from an area covered by intermediate snow (8–15 cm) using a 9 cm internal diameter core barrel (Kovacs Mark II). In some occasions where snow cover appeared very variable, separate sets of samples were taken from areas with high (<15 cm) and low (<5 cm) of snow. Natural heterogeneity in sea ice core protists biomass [34] was overcome by collecting 3 replicate samples, each consisting of 1–6 pooled ice core bottom slices for each sampling day. All sea ice cores were melted with addition of 0.7 μm filtered seawater (9 parts FSW to 1 part melted ice) to minimize osmotic stress on the microbial community during melting [35]. Once melted, ice core samples were filtered (GF/F), filters were wrapped in aluminum foil and stored in liquid nitrogen. Two additional ice cores were obtained for each sampling date: one to measure the ice temperature and salinity to estimate brine volume, the other for analyzing inorganic nutrients (see below). For total dissolved inorganic carbon (DIC) in sea ice, ice cores were collected using the same ice corer (Kovacs, Ø = 0.09 m), where the full length ice cores were directly placed in long-sleeve plastic bags and put into a −20 °C freezer for short-term storage (few days), and further transport to the laboratory at the University Centre in Svalbard (UNIS, Longyearbyen). In the laboratory, the ice cores were cut into 10 cm sections, where only the bottom 10 cm of the bulk sea-ice (hereafter referred to as sea ice) was used. The ice pieces were immediately transferred to gastight Tedlar bags to initiate the ice melting as soon as possible. The sea-ice samples were thawed in a cool and dark place with a melting time of approximately 24–48 h. Samples from the water column were taken with a Niskin bottle from discrete depths (5, 10, 15, 25, and 50 m), in addition, surface water from directly underneath the sea ice was sampled with a manual hand pump. The water samples were kept cold and dark, and filtered within a few hours after each field trip;

further sample analysis procedures were identical to sea ice samples. Due to low biomass in the deeper samples, samples from several depths had to be pooled for trophic marker analysis in order to obtain sufficient biomass.

2.3. Organic Carbon Analysis

Particulate organic carbon (POC) and nitrogen (PON) of sea ice algae were measured after filtration onto pre-combusted (4 h, 450 °C) GF/F filters (Whatman). Filters were stored at −20 °C and soaked with 200 mL 0.2 M HCl (Merck) to remove inorganic carbon. Filters were dried for at least 12 h at 60 °C prior to sample preparation. Analysis was performed using a CHNS-O elemental analyzer (Euro EA 3000, HEKAtech) which was calibrated using acetanilide standards. Contents of POC and PON were corrected for blank measurements and normalized to filtered volume and cell densities to yield cellular quotas.

2.4. Lipid Analysis

For lipid analysis, 9-octyl-8-heptadecene (10 μL; 0.5 μg mL^{-1}) internal standard was added to filters in combination with nonadecanoic acid (10 μL; 1 mg mL^{-1}) for quantification of HBIs and fatty acids respectively from sea ice (36–145 mL filtered). Filters were then saponified (5% KOH; 70 °C; 60 min), after which non-saponifiable lipids (including HBIs) were extracted with hexane (3 × 2 mL) and purified by open column chromatography (SiO$_2$; 3 column volumes of hexane). Combined hexane extracts were dried using N$_2$. Fatty acids were obtained by adding concentrated HCl (1 mL) to the saponified solution (after extraction of non-saponifiable lipids) and re-extracted with hexane (3 × 2 mL). Identification of HBIs was achieved following analysis by selective ion monitoring (SIM; *m/z* 350.3, *m/z* 348.3, and *m/z* 346.3; limit of detection = 1 ng L^{-1}) using a Shimadzu QP2010 gas chromatograph coupled to a QP2020 quadrapole EI mass spectrometer (GC-MS; HP5ms; [36]). Comparison of HBIs in sample extracts to the retention index and mass spectra obtained from standard extracts and literature provided unambiguous identification. Molecule structures and nomenclature of the analyzed HBI compounds are summarized in Figure S1. Fatty acids were derivatized to methyl esters by the addition of HCl:MeOH (1 mL; 1:9) and heating (70 °C; 60 min). Fatty acid methyl esters were re-extracted with hexane (3 × 2 mL) and analyzed at the Alfred Wegener Institute (AWI) using a gas chromatograph (GC-6890N, Agilent Technologies) equipped with an automatic sampler fitted with a J&W DB-FFAP column (60 m, 0.25 mm internal diameter, 0.25 μm film). Inlet and FID detector temperatures were set at 250 and 260 °C, respectively. Helium was used as a carrier gas in constant flow mode at an average linear velocity of 25 cm sec^{-1}. Oven temperature started at 80 °C for 2 min, then increased following two ramps (up to 160 °C at 20 °C min^{-1}, and then up to 240 °C at 2 °C min^{-1}) with a final hold time of 20 min at 240 °C. Individual fatty acids were identified by comparing relative retention times with those of a known standard mixture derived from Arctic and Antarctic copepods. For quantification, HBI abundances were normalized according to a response factor (Belt et al. 2012), and both HBIs and fatty acids were further normalized to quantities of internal standards and sample mass or volume as required. Quantification was carried out on peaks with s/n = ≥3.

2.5. Bulk Stable Isotope Analysis

All samples for isotope compositions were analyzed using an elemental analyzer (Flash 2000, Thermo Scientific, Milan, Italy) coupled to an isotope ratio mass spectrometer (Delta V Plus with a Conflo IV interface, Thermo Scientific, Bremen, Germany). Analyses were conducted at the Littoral, Environment and Societies Joint Research Unit stable isotope facility (University of La Rochelle, France). Results are expressed in the δ notation as deviations from standards (Vienna Pee Dee Belemnite for δ^{13}C and N2 in air for δ^{15}N) following the formula: δ^{13}C or δ^{15}N = ((R$_{sample}$/R$_{standard}$) − 1) × 10^3, where R is ^{13}C/^{12}C or ^{15}N/^{14}N. Prior to isotope analysis of δ^{13}C, carbonates were removed by adding a few drops of HCl 0.2 mol L^{-1} until cessation of bubbling. Subsequently, samples were dried at 60 °C. Calibration was done using reference materials (USGS-24, -61, -62, IAEA-CH6, -600 for carbon; USGS-61, -62,

IAEA-N2, -NO-3, -600 for nitrogen). The analytical precision of the measurements was <0.15‰ for carbon and nitrogen based on analyses of USGS-61 and USGS-62 used as laboratory internal standards. This method allows obtaining $\delta^{15}N$ values in parallel, but we will report on $\delta^{13}C$ values only.

2.6. Compound-Specific Isotope Analysis of Fatty Acids

The $\delta^{13}C$ isotopic composition in FAs was measured using a Thermo gas chromatography-combustion isotope-ratio mass spectrometry (GC-c-IRMS) system (Thermo Scientific) (see [37]). For each analytical run, 2 reference gas pulses were used for data calibration at the start and at the end, together with the internal standard 23:0 FA methyl ester (FAME) ($\delta-32.50‰$, Pee Dee Belemnite (PDB)). The chromatographic peak areas and carbon isotope ratios were obtained with the instrument-specific software (Isodat 3.0), and the certified reference standards 14:0 and 18:0 FAME (Iowa University) were used with known δ^{13}-values for further calculations.

2.7. Sea Ice Algae Taxonomy

Subsamples of 100–200 mL were fixed with a mixture of glutaraldehyde and Lugol's solution (both 2% final concentration) for qualitative and quantitative analyses. Taxonomic identification of sea ice algal species was carried out on each ice core sample using the Utermöhl method [38]. As sea ice samples were so dense, 0.5 mL of sample were suspended in 9.95 mL of artificial seawater (to ensure uniform settling on the bottom of the chamber), and then a 10 mL Utermöhl chamber was used. Species identification and countings were carried out using an inverted microscope (Nikon TE-300 under magnifications of 100× and 600×), equipped with phase and interference contrasts and a picture acquisition system (NisElements BR). Taxa >20 μm were counted on the entire chamber surface under 100× magnification. The cells were counted in an ocular photomask frame of a known area along the transect crossing the bottom chamber surface. Cells <20 μm were counted under 400–600× magnification on 3 parallel transects. Biovolume calculations were done based on stereogeometric shapes measurements and calculated according to the HELCOM Phytoplankton Expert Group (PEG) biovolume spreadsheet. Conversions to biomass were done according to Menden & Deuer [39]. More detailed examination of certain taxa was achieved by dry-mounting sub-samples of cleaned (10% HCl; 70 °C for 30 min and 3 × 10 mL Milli-Q washes) cells and examination using a JEOL 7001F scanning electron microscope. In addition, diatoms belonging to the *Haslea* genus with known ability to produce IP$_{25}$, specifically, were identified based upon general morphological dimensions in addition to features considered characteristic of the genus including, for example, the presence of external longitudinal strips over many areolae, with intervening continuous slits.

2.8. Determination of Inorganic Nutrient Concentrations

Ice core sections for nutrient analysis were thawed without addition of filtered seawater in the dark within appx. 24 h. Nutrient samples were filtered using acid washed syringes (10% HCl, 48 h) and GF/F filters. Samples were stored in 15 mL acid washed Falcon tubes at −20 °C until further analysis. After thawing, the concentrations of nitrate, phosphate, and silicate were measured colorimetrically on a QuaAAtro autoanalyzer (Seal Analytical, Mequon, WI, USA) using internal calibrations and CRMs (KANSO, Osaka, Japan) for quality control.

2.9. Determination of Total Dissolved Inorganic Carbon

The thawed sea ice was transferred to 250 mL borosilicate glass bottles. Saturated mercuric chloride was added to the melted sea ice (60 μL for 250 mL) to halt biological activity. Samples were analyzed for DIC at the Institute of Marine Research, Tromsø, Norway. Analytical methods for DIC determination in seawater samples are described in [40]. DIC was determined using gas extraction of acidified samples followed by coulometric titration and photometric detection using a Versatile Instrument for the Determination of Titration carbonate (VINDTA 3C, Marianda, Germany). Routine analyses of Certified Reference Materials (CRM, provided by A. G. Dickson, Scripps Institution of Oceanography,

USA) ensured the accuracy and precision of the measurements. The average standard deviation from triplicate CRM analyses was within ±1 μmol kg^{-1}.

2.10. Determination of Chlorophyll a (Chl a)

Samples for Chl a determination were filtered onto GF/F filters (Whatman, Maidstone, UK) using a gentle vacuum, shock frozen in liquid nitrogen, and stored at −80 °C until further analysis. For analysis filters were extracted in 10 mL methanol for 24 h at +4 °C in darkness and measured on a 10-AU-005-CE Fluorometer (Turner Designs, San Jose, CA, USA).

2.11. Statistical Analysis

All data analysis was conducted using R 3.5.0 (R Core Team 2018: R: a language and environment for statistical computing. R Foundation for Statistical Computing, Vienna, Austria. URL: https://www.R-project.org/). Compositional bar charts were used to show the changing species composition across the transect, and also, specifically for station MS, the changing composition over the period 4 April–2 May 2017. Similarly, scatter plots were used to show different variables along the transect, and again specifically for station MS, their values for the short time series. To compare the ice and pelagic samples for several variables at the same time, either canonical correspondence analysis (CCA, for compositional variables) or redundancy analysis (RDA, for interval-scale variables) was used, where the solution was constrained to show the ice-pelagic contrast on the first dimension. The package "vegan" (Oksanen J, Blanchet FG, Friendly M, Kindt R, Legendre P, McGlinn D, Minchin PR, O'Hara R.B., Simpson GL, Solymos P, Stevens HH, Szoecs E, Wagner H. 2019. vegan: Community Ecology Package. R package version 2.5–6, https://CRAN.R-project.org/package=vegan (last accessed 30 March 2020)) was used to conduct a multivariate permutation test on this dimension, thereby testing the ice-pelagic difference in a multivariate framework. To further investigate the correlation between different trophic markers and nutrient concentrations or stoichiometry, Spearman rank correlations were computed due to the nonlinear relationships observed in the scatterplots of the variables. The *p*-values for the correlations are estimated using a distribution-free permutation test [41], as implemented in the function perm.cor.test in the R package jmuOutlier (Garren ST 2019. jmuOutlier: Permutation Test for Nonparametric Statistics. URL https://CRAN.R-project.org/package=jmuOutlier). Because of multiple testing, the Benjamini-Hochberg step-up procedure was used to avoid false positives at the overall *p* = 0.05 level [42,43].

3. Results

3.1. General Physical Situation, Development of Chl a, Nutrients and C:N Ratios along the Transect and over Time

Sea ice algae abundance and taxonomy were studied from early March to early May, but only from April onwards did biomass concentrations become high enough to measure all trophic markers in sea ice samples. Sea ice thickness varied from 30 to 50 cm, and snow cover on top of the ice was between 0 and 27 cm. For a more detailed description of the general situation, including algal physiology see [44]. In short, highest sea ice Chl a concentrations at the main study station (MS) were measured on April 23rd with up to 260 μg L^{-1}, whereas 160–170 μg Chl a L^{-1} were measured on 29th April and 2nd of May (Table 1). With respect to POC concentrations, the highest concentrations were found on the 23rd of April and 2nd of May, with 8–10 mg L^{-1}. Interestingly, the POC:Chl a ratio clearly reflected the impact of increased light under lower snow cover, and increased from 23 (23/4, high snow cover) to 93 (2/5, no snow) within only two weeks. Along the transect, Chl a concentrations varied between 120 and 190 μg L^{-1}, with only VMF2 being much lower (44 μg L^{-1}), while POC concentrations ranged from 2.5 (VMF2) to 13.7 mg L^{-1} (IS). Concentrations of diatom lipids (Σ of 16:1(n-7), C16 PUFAs, 20:5(n-3)) were highest at the shallow IS station (178 ng mL^{-1}), and lowest at MS (25 ng mL^{-1}). Normalized to POC, however, the highest amounts were found at VMF2 (39 ng (μg POC) mL^{-1}). Nutrient concentrations in sea ice were declining over time – in particular for nitrate and silicate.

Along the transect, the highest silicate concentrations were measured in the areas with shallowest water depth, namely stations IS and IM, with 1.6 and 1.5 µmol L^{-1}, respectively. At other locations concentrations were <1 µmol L^{-1}. At station IS, the highest nitrate concentration in ice was detected (16 µmol L^{-1}), followed by IM (5.2 µmol L^{-1}) and MS (4.2 µmol L^{-1}, Table 1). Dissolved inorganic carbon (DIC) concentrations were measured only at MS, VMF1, and VMF2. At the end of April, DIC was highest at the MS station (344 µmol kg^{-1}) and decreased to its lowest values at VMF2 (319 µmol kg^{-1}). Time series measurements of environmental parameters conducted at sampling station MS showed rather similar patterns. Highest DIC concentrations of 387 µmol kg^{-1} were observed at the beginning of April and then decreased, most rapidly between 23rd of April to 2nd of May, from 369 to 337 µmol kg^{-1}. The lower DIC coincided with decreasing nitrate concentrations. Nitrate first only declined slowly from early April (approx. 4 µmol L^{-1}) to the 23rd of April (3 µmol L^{-1}). Under high snow cover, even concentrations of 14 µmol L^{-1} were measured on that day, maybe indicating a slower sea ice algal bloom development under high snow cover. However, on the 2nd of May, nitrate was substantially reduced to concentrations below 1 µmol L^{-1}. Interestingly, a similarly strong gradient of nitrate concentrations was found along the transect, ranging from 15–16 µmol L^{-1} at the shallowest station (IS) to <0.2 µmol L^{-1} at VMF2 (Table 1). Silicate concentrations at most of the stations and sampling events were rather depleted, well below 1 µmol L^{-1}, with the only exception being the shallowest area of the transect (stations IS and IM), where values between 1.5 and 2 µmol L^{-1} were found. Phosphate concentrations varied between 0.3 and 1.5 µmol L^{-1} without any clear spatial or temporal trend.

Molar ratios of POC to PON. Particulate carbon to nitrogen ratios displayed a distinct spatial pattern, with values around 6–7, close to Redfield proportions, at the three innermost stations (IS, IM, MS), and clearly higher values at VMF1 and VMF2 (i.e., almost twice as high, Figure 2A). This corresponds well with the different nitrate concentrations measured in sea ice (see Table 1, Figure 2A), where stations VMF1 and VMF2 were almost completely depleted for nitrate. Again, this spatial pattern resembled the main trend in the temporal development at MS, with a development towards nitrated depletion and increased POC:PON ratios in early May, even more pronounced at the sampling location with little to no snow coverage (Figure 2B).
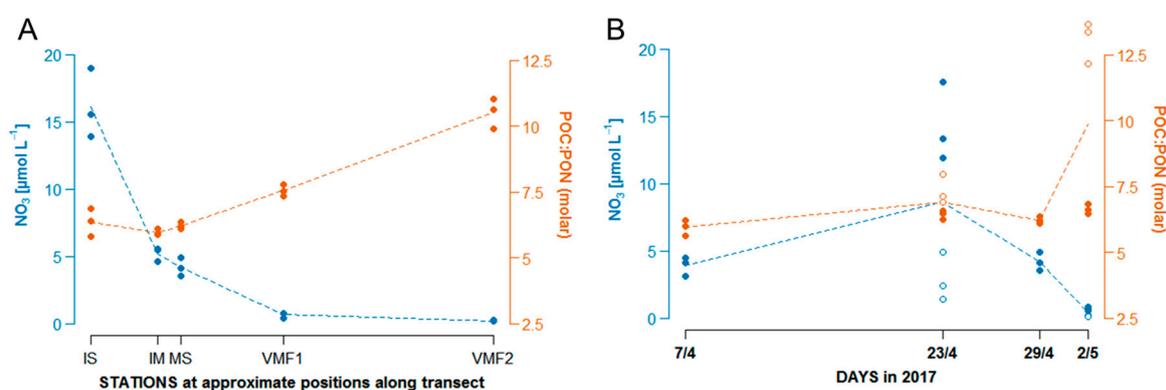

Figure 2. Nitrate concentrations (µmol L^{-1}) and molar ratios of POC to particulate organic nitrogen (PON) along the transect (**A**) and changing over time (**B**). In the time series data, localities with low and high snow were sampled specifically on two occasions (23/4 and 2/5), clearly displaying distinct C:N ratios and nutrient concentrations (open symbols: low snow, filled symbols: high snow). Trendlines were inserted based on overall average values of all samples taken on a given day (n = 3–6).

Table 1. Physico-chemical and biological characteristics of bottom sea ice (0–3 cm) sections with respect to nutrients, dissolved inorganic carbon, DIC, temperature, salinity, algal biomass (measured as particulate organic carbon, POC, and chlorophyll a, Chl a), as well as lipids along the transect, and for the time series. Shown are means and SD (n = 3).

Station.	Date	Snow	IP_{25} (pg mL^{-1})			Σ-Diatom FA (ng mL^{-1})			Σ-Diatom FA: POC (ng/μg mL^{-1})			C (POC) (μg L^{-1})			Chl a (μg L^{-1})			Salinity			T_{ice} (°C)			PO_4 μmol/L			SiO_2 μmol/L			NO_3 μmol/L			DIC (μmol/kg)
			Mean	±	SD	Mean	±	SD	Mean	±	SD	Mean	±	SD	Mean	±	SD	Mean	±	SD	Mean	±	SD	Mean	±	SD	Mean	±	SD	Mean	±	SD	
Transect																																	
IS	28.4.17	NA	50.5	±	11.0	178.0	±	82.0	12.7	±	4.9	13,671.4	±	2781.8	190.4	±	19.8	8.7	±	2.5	−1.9	±	0.0	1.1		1.0	1.5	±	0.9	16.2	±	2.6	
IM	28.4.17	NA	40.5	±	7.1	60.1	±	20.0	11.5	±	1.2	5216.7	±	1411.4	119.5	±	12.8	5.3	±	0.8	−1.6	±	0.0	1.1		0.2	1.6	±	0.4	5.2	±	0.5	
MS	29.4.17	NA	31.3	±	10.5	25.1	±	1.3	5.4	±	0.3	4674.0	±	41.7	167.9	±	17.6	7.2	±	1.3	−1.7	±	0.0	1.3		0.6	0.9	±	0.3	4.2	±	0.7	344
VMF1	30.4.17	NA	2.9	±	0.6	116.1	±	13.0	12.0	±	0.6	9742.7	±	1314.5	181.5	±	7.9	12.7	±	0.2	−1.7	±	0.1	1.5		0.8	0.3	±	0.3	0.6	±	0.2	331
VMF2	30.4.17	NA	0.5	±	0.3	97.4	±	41.7	38.8	±	2.1	2542.8	±	1174.2	44.5	±	17.8	7.9	±	0.0	−1.5	±	0.0	0.3		0.0	0.2	±	0.1	0.2	±	0.0	319
Time series																																	
MS	7.4.17	NA	6.2	±	5.7	13.1	±	8.4	5.3	±	1.0	2330.6	±	1039.3	68.8	±	9.8	12.2	±	0.7	−1.6	±	0.0	0.4		0.1	0.3	±	0.1	3.9	±	0.7	387
MS	23.4.17	High snow	10.9	±	3.7	32.1	±	2.4	5.4	±	0.6	5923.3	±	333.2	259.2	±	20.1	14.0	±	0.8	−2.0	±	0.1	0.8		0.1	0.5	±	0.2	14.2	±	2.8	
MS	23.4.17	Low snow	22.1	±	2.7	141.1	±	21.1	16.2	±	2.6	8938.2	±	2377.1	252.3	±	63.5	14.9	±	0.7	−1.9	±	0.0	1.4		0.3	0.7	±	0.2	3.1	±	1.8	369
MS	29.4.17	NA	31.3	±	10.5	25.1	±	1.3	5.4	±	0.3	4674.0	±	41.7	167.9	±	17.6	7.2	±	1.3	−1.7	±	0.0	1.3		0.6	0.9	±	0.3	4.2	±	0.7	344
MS	2.5.17	No snow	10.0	±	1.0	477.2	±	24.7	49.4	±	4.1	9666.8	±	298.3	105.8	±	8.3	12.2	±	0.3	−1.8	±	0.1	1.5		0.2	0.5	±	0.2	0.2	±	0.0	337
MS	2.5.17	High snow	9.0	±	2.7	99.6	±	42.8	12.7	±	2.3	7632.1	±	1906.9	161.4	±	6.8	12.3	±	0.1	−1.7	±	0.1	1.3	±	0.3	0.3	±	0.1	0.7	±	0.2	

3.2. Species Composition

Results from the analysis of ice algal species composition along the transect (available for all stations apart from VMF2) revealed that diatoms (Bacillariophyceae) accounted for 76–89% of the total algal biomass at all stations (Figure 3). Diatoms almost exclusively comprised pennate species, with the vast majority being typical ice-associated species, without any clear spatial trend. There was some variability between replicates at sampling sites and sampling stations, with Chrysophyceae being the second most important group at the shallow coastal site (IS station) and accounting for 17%. At the remaining three stations, dinoflagellates were the algal group that was second most dominant, accounting for 13–20% of total algal biomass. Prymnesiophyceae were only found at VMF1 (about 4% of total biomass). Other groups represented only very minor contributions to the overall algal biomass (Figure 3A). Following the species composition data from early April to early May at the main station (MS), similar patterns are visible: Bacillariophyceae account for 70 to >95% of the total algal biomass, with one notable exception being the sample taken on the 2nd of May under low/no snow conditions (Figure 3B). Here, the sympagic Euglenozoa *Anisonema* sp. accounted for almost 25% of the total biomass. Within the Bacillariophyceae, pennates were by far most abundant, and classified ice-associated species outnumbering pelagic ones (50–87% vs. 3–12%).

(A)
            (B)
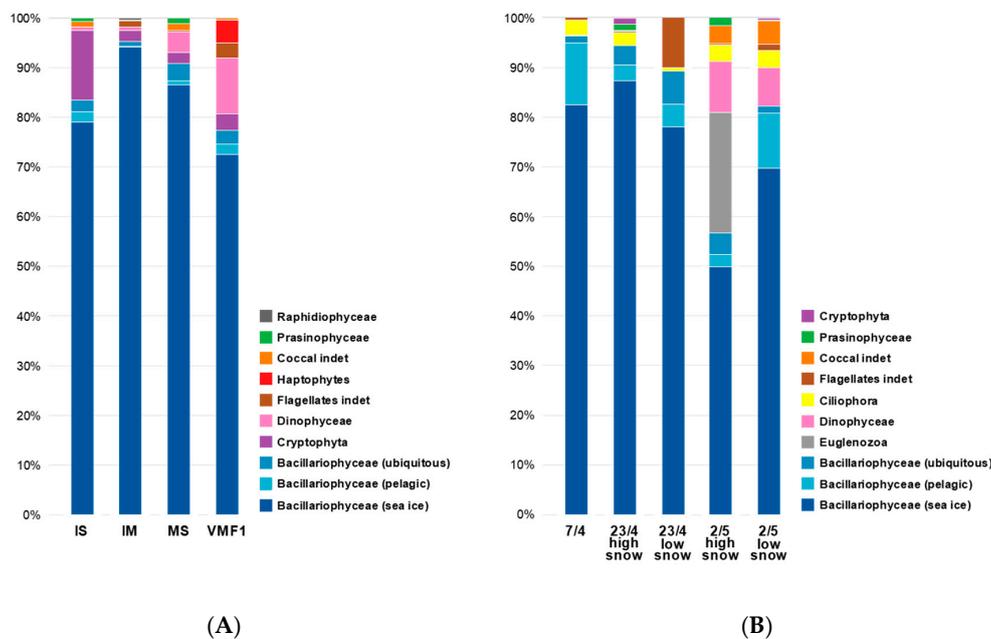
Figure 3. Taxonomic composition of microalgae in sea ice samples taken along the transect (**A**), and over time at MS (**B**). Shown are % carbon biomass data (mean of 1–3 replicates), converted from abundances via biovolume calculations. Complete species lists are provided in the supplementary material, Table S1A,B. All transect stations were sampled within 48 h (28–30 April).

3.3. Variability of Ice Algal Biomarkers on Short Spatial and Temporal Scales

All sea ice algal trophic markers displayed a remarkable variability along the sampling transect in the inner part of Van Mijenfjorden.

3.3.1. FATM

Diatom fatty acid markers (16:1(n-7), 16:4(n-1), and 20:5(n-3)) were detected in all samples collected along the transect, but with different relative abundances. In communities collected in shallow areas close to shore, fatty acid composition consisted of 18% 20:5(n-3) and up to 6% 16:4(n-1), while samples collected at the mid-fjord stations VMF1 and VMF2 were characterized by almost 50% 16:1(n-7), and only 4.5–8% 20:5(n-3), and 0.7–1.6% 16:4(n-1) (Figure 4A, Table S2). When summarizing all C_{16}

PUFAs (a measure that is often used as a diatom indicator), a reduction by 80% was found between the shallowest and the deepest areas. Overall PUFAs were 50% lower at VMF1 compared to the innermost two stations (IS and IM), and about 66% lower at VMF2. Very similar changes in fatty acid composition were also found over time at MS station, with equally high percentages of 16:1(n-7) on the last sampling date (Figure 4B). PUFAs decreased substantially over time, 20:5(n-3) accounting for up to 12% of all fatty acids in early April, but for only less than 6% in early May, and the corresponding values for 16:4(n-1) were 6 vs. 2% (Figure 4B, Table S2).
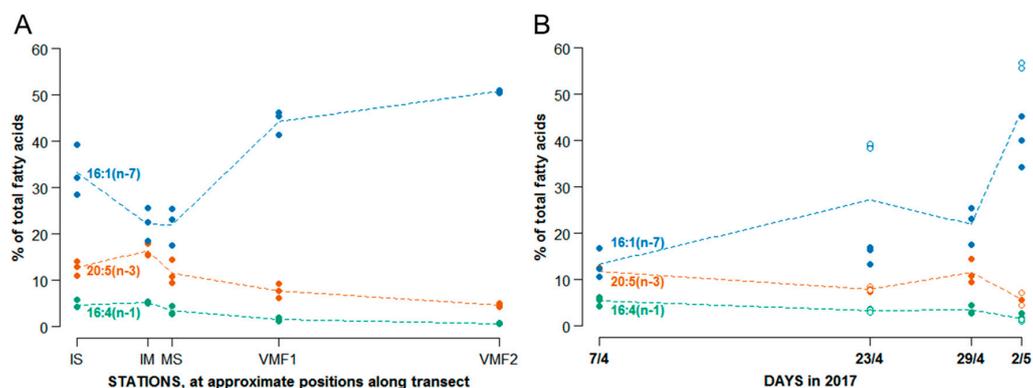
Figure 4. Relative abundances (%) of the most important diatom fatty acid trophic markers, 16:1(n-7), 16:4(n-1) and 20:5(n-3) along the transect (**A**), and measured at MS over time (**B**).

3.3.2. HBIs

Along the transect, highest values of the ice algae biomarker IP_{25} (normalized to POC) were detected at IM and MS station (on average 0.007–8 *w/w*), about 50% of these values at the shallowest station, and very little at mid-fjord stations VMF1 and VMF2 (Figure 5). Without normalization, the highest IP_{25} concentrations were found at the shallowest station IS with 50.5 pg mL^{-1}, decreasing towards VMF2 where only 0.5 pg mL^{-1} was found (Table 1).
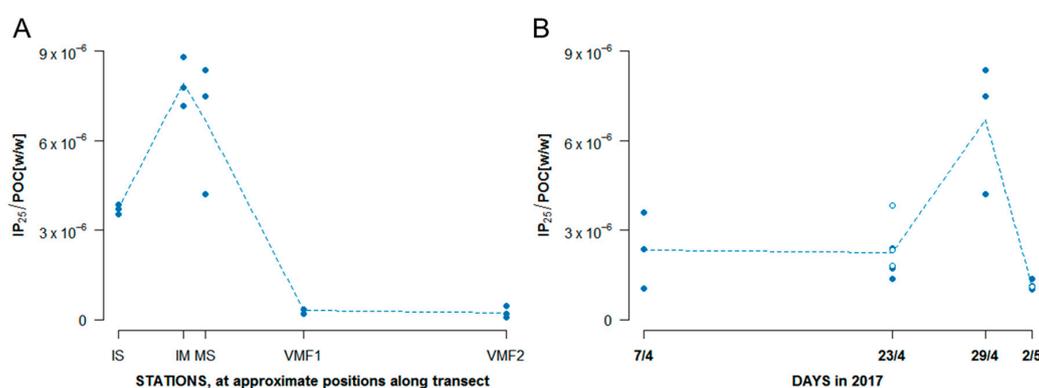

Figure 5. IP_{25} normalized to POC (*w/w*) along the transect (**A**) and changing over time at MS station (**B**). Open symbols depict low snow cover (less than 5 cm), filled symbols intermediate-high snow cover.

3.3.3. Stable Isotope Ratios

Stable isotope ratios in particulate organic carbon (δ^{13}C POC) along the transect ranged from −23 to −22‰ at the shallowest near-shore stations to −19 to −18‰ at VMF1 and VMF2, respectively. For single diatom marker fatty acids, δ^{13}C values were considerably higher (i.e., more enriched) at VMF2 than any other station, with some variability between the different fatty acids, but an overall consistent pattern (Figure 6A, Table S3). δ^{13}C for 16:1(n-7), 16:0, and 20:5(n-3) were more enriched at VMF1 compared to MS, IM, and IS, whereas no such difference was found for δ^{13}C 16:4(n-1). Stable isotope ratios of bulk POC measured over time at MS station were rather stable throughout

April (21–23‰), with increasing (more enriched) δ^{13}C values only on the very last day of sampling in early May (2/5), in particular at the site with little to no snow coverage (15‰, Figure 6B, Table S3).
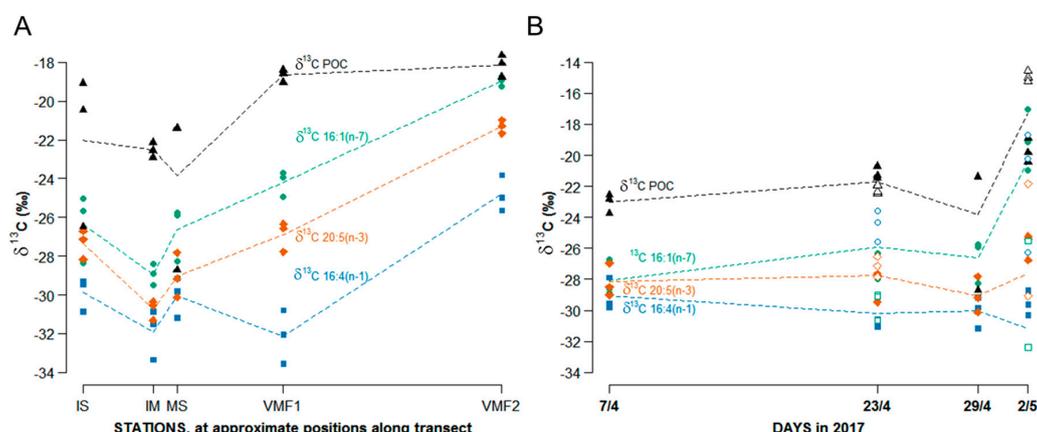

Figure 6. δ^{13}C for bulk POC (in black) and single diatom marker FAs (in color), determined along the transect (**A**), and measured at MS over time (**B**). Open symbols indicate sampling sites with very little snow cover (<5 cm), filled symbols sites with intermediate to high snow coverage.

3.4. Comparing the Ability of Different Markers to Distinguish between Algae Collected in Sea Ice vs. Water Column

During sampling we observed the co-occurrence of a phytoplankton spring bloom that peaked almost simultaneously with the ice algal bloom in Van Mijenfjorden in late April/early May 2017 [44]. We used this opportunity to test whether it was possible to distinguish samples taken from the lowermost section of ice cores (0–3 cm) from those collected from different depths in the water column based on the lipid and stable isotope composition. To this end, we carried out a CCA where the first dimension was constrained to reflect the distinction between sea ice vs. water samples in the best possible way. This was done separately for each biomarker approach; complete fatty acid composition (Figure 7), HBIs (Figure 8), and compound specific δ^{13}C of individual fatty acids (Figure 9).
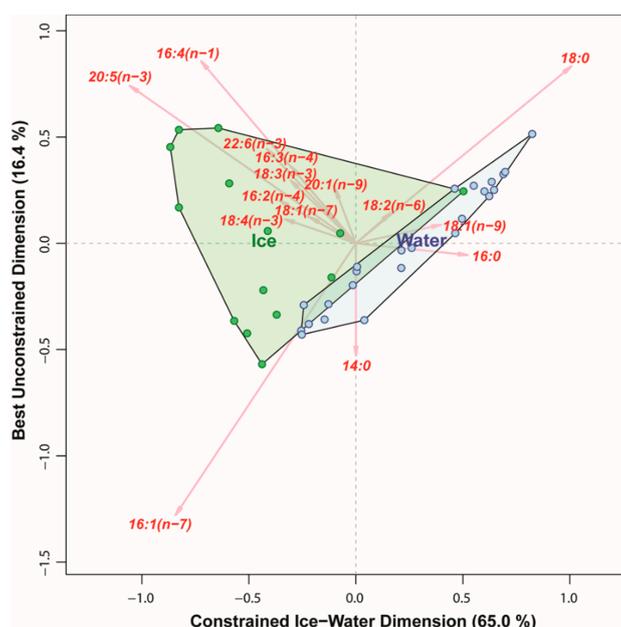
Figure 7. Distinguishing particulate organic matter (POM) samples from Van Mijenfjorden (April 2017–May 2017) by means of their relative fatty acid composition (%), using a canonical correspondence analysis (CCA). Every dot represents a sample, green are samples from 0–3 sections of sea ice, in blue are samples taken from the water column.
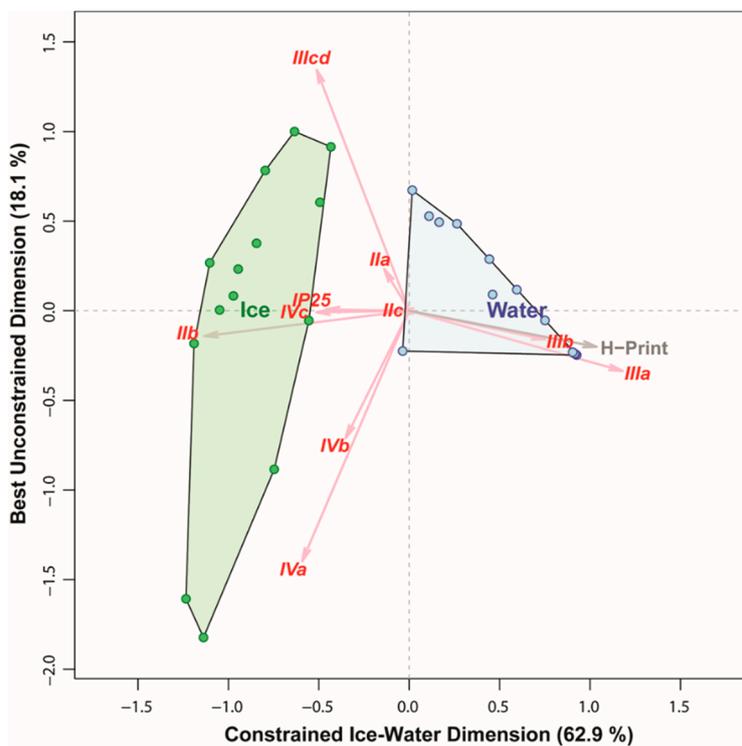
Figure 8. Distinguishing POM samples from Van Mijenfjorden (April 2017–May 2017) based on their HBI (highly branches isoprenoids) composition, using a CCA. Every dot represents a sample, green are samples from 0–3 sections of sea ice, in blue are samples taken from the water column.
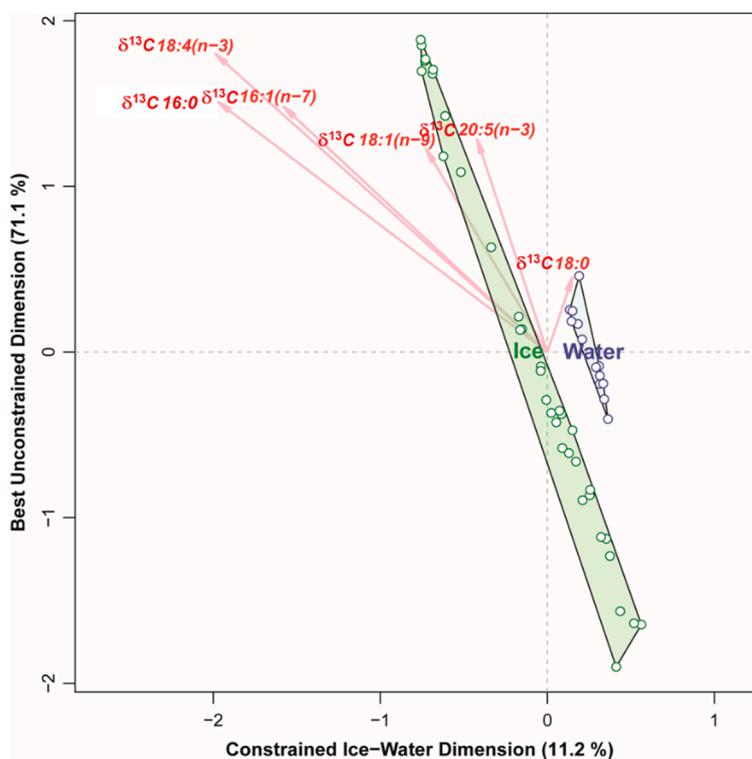
Figure 9. Distinguishing POM samples from Van Mijenfjorden (April 2017–May 2017) based on $\delta^{13}C$ of individual fatty acids, using an RDA. Every dot represents a sample, green are samples from 0–3 sections of sea ice, in blue are samples taken from the water column.

Distinction based on fatty acid composition resulted in a first constrained axis with very high explanatory power (65% of total variability), but did not yield a complete separation of samples within the first two dimensions, with a number of water column samples being grouped close to sea ice samples (Figure 7). Nonetheless, most of the sea ice samples had higher percentages of PUFAs than those from the water column. The HBI-based multivariate analyses yield a first axis with a similarly high explanatory power (63% of total variability) but, in contrast to FAs, provided a very clear and consistent distinction between sea ice and water samples (Figure 8) within the first two dimensions. Sea ice samples had relatively higher concentrations of sea ice diatom HBIs; IP_{25} as well as the HBIs IIb and IVc relative to samples of pelagic origin. When comparing all samples based only on the $\delta^{13}C$ of individual fatty acids, the variability explained by the ice-water contrast on the first axis decreased to 11.2% of the total (Figure 9). This reflected the enormous variability of $\delta^{13}C$ values within the sea ice samples which far exceeded the difference between pelagic and sea ice samples. In contrast, pelagic samples showed much less variability in their $\delta^{13}C$ values.

4. Discussion

4.1. Variability of Trophic Markers—And How This Relates to Environmental Conditions

Our results document a considerable variability in all studied trophic markers on short temporal and spatial scales. This is in line with previous findings (e.g., [17,28,30]), but we are, for the first time, able to show this systematically in a comparison including four different marker approaches in one dataset. In order to use trophic markers reliably and in a scientifically sound way, one needs to understand their biochemical nature and acknowledge the intrinsic coupling of growth conditions and physiological state of microalgae with their trophic marker baseline signal. It was remarkable to see how well the spatial variability of both nutrient concentrations and trophic markers resembled their changes over time: starting from early April (similar to the shallowest transect stations IS, IM) to early May (resembling VMF1 and VMF2, see Figures 4–6). Hence, we conclude that at least one underlying factor explaining the spatial variability along the transect corresponds to a delay in bloom development at the shallowest stations. This is reflected in the replete nutrient concentrations at these stations. The lower dissolved inorganic carbon (DIC) concentrations at the outer stations relative to the inner one (MS) also indicated an earlier bloom start at the former (i.e., a further progressed bloom development at the time of sampling).

During bloom succession, several environmental parameters change simultaneously (e.g., availability of inorganic carbon and nutrients, light, temperature, etc.), and it is therefore impossible to completely disentangle their individual impact on trophic marker qualities from field observations only. However, our results point towards a key role of nutrient limitation that led to profound changes in trophic marker signals, as the samples that differ strongest from each other with respect to their fatty acid composition or their isotopic signal originate from samples with contrasting nutrient concentrations. Nutrient limitation is reflected in low absolute concentrations of the limiting nutrients in the water, but also, indirectly, in the stoichiometric ratios of POC:PON from particulate sympagic matter deviating from Redfield-ratios. We therefore analyzed the correlations of our trophic marker compounds with (a) nitrate concentrations, (b) silicate concentrations, and (c) C:N ratios of POM. In total, we found 11 significant or highly significant correlations, four of which were with nitrate concentrations, one with silicate (IP_{25} normalized to POC), and six with C:N ratios (Table 2). The only two markers tested that were not significantly correlated with any of these three parameters were the compound-specific $\delta^{13}C$ values for the diatom PUFAs 16:4(n-1) and 20:5(n-3). The time series data of these two markers were also the ones hardly increasing at all (Figure 6B), although they were found to be markedly different at station VMF2 compared to all other stations in the transect (Figure 6A). Unfortunately, we do not have complete datasets for all other environmental variables—and in particular DIC - whose impacts could have been tested in a similar manner, even though strong autocorrelation between some of them likely would complicated this type of analyses. But the highly significant

positive correlations of 16:1(n-7) and $\delta^{13}C$ of 16:1(n-7) with C:N ratios, and nitrate concentrations (Table 2), strengthen our hypothesis about a key role of this particular fatty acid in metabolic changes towards lipid accumulation during unfavorable conditions. Percentages of fatty acids were more strongly correlated with nitrate concentrations and C:N ratios compared to their specific stable isotope ratios, while $\delta^{13}C$ of bulk POC was highly significantly correlated with C:N ratios, but not with nutrient concentrations (Table 2). In [44] we investigated the correlation between nutrients and stoichiometric ratios on algal photophysiology, such as photosynthetic efficiency, also known as maximum quantum yield of photosynthesis. This measure responds extremely rapidly to changes in the environment and in sea ice algae we found the strongest correlation with ambient concentrations of inorganic nutrients, as well as light. Lipid- and isotope-based marker signals, on the other hand, react on slower timescales than photophysiology, since they reflect no instantaneous acclimation reactions but rather alterations in metabolic patterns. We consider this being the reason for them being most strongly correlated with altered C:N ratios, that also reflect a more consolidated "effect" of nutrient limitation.

Table 2. Correlations between selected biomarkers and nutrient concentrations. The correlations marked ** are highly significant ($p < 0.005$), those marked * are significant ($p < 0.02$). False positives are avoided using the Benjamini-Hochberg step-up procedure, with overall significance level of 0.05.

Biomarkers	NO$_3$ (µmol L^{-1})	SiO$_2$ (µmol L^{-1})	C: N (molar)
IP$_{25}$/POC	0.770 *	0.802 **	−0.782 *
16:1(n-7)	−0.794 **	−0.261	0.903 **
16:4(n-1)	0.758 *	0.462	−0.939 **
20:5(n-3)	0.709	0.669	−0.782 *
$\delta^{13}C$ POC	−0.673	−0.438	0.891 **
$\delta^{13}C$ 16:1(n-7)	−0.733 *	−0.498	0.818 **
$\delta^{13}C$ 16:4(n-1)	0.006	−0.486	−0.188
$\delta^{13}C$ 20:5(n-3)	−0.370	−0.608	0.418

4.2. Fatty Acid Trophic Markers (FATM)

A substantial decrease in the relative amount of PUFAs during the course of phytoplankton and sea ice algal spring blooms in Arctic waters has been shown before [16,17], and was attributed primarily to deteriorating environmental conditions, such as declining nutrient concentrations. For sea ice algae specifically, however, high irradiances were also found to decrease the relative amount of PUFAs, as we saw in the current study when comparing sites with high vs. low snow cover. This was also evident in an earlier field study in Rijpfjorden 2007 [16]. Experimental studies with diatom cultures in outdoor aquaria and in situ incubations further confirmed this observation [18,45]. A recent comparison of physiological responses to sudden high light stress in a dominant sea ice diatom with a typical pelagic diatom indicates that the sea ice diatom was strongly negatively affected by high light stress, and hardly recovered over several days [46], whereas its pelagic counterpart was able to successfully acclimate to the new light levels within less than three days. Molecular analyses point towards differences in the antioxidant reaction scheme between the two algal groups, with the sea ice diatom having a less efficient functional response in place. This could potentially explain the decrease in relative PUFA content, as fatty acids with a higher number of double bonds get more readily oxidized [47,48]. This process is strongly enhanced in damaged or decaying cell material which is also found more frequently during late bloom stages. Nutrient depletion also induces changes in fatty acid composition of microalgae, with a marked decrease in PUFAs compared to nutrient replete conditions, and a strong increase in percentage of 16:1(n-7) under nitrate depletion [13], probably indicative for increased storage lipid formation (Leu et al. unpublished data), which was also found in experimental studies [49,50]. This interpretation is further strengthened by the observation that samples with the highest percentage

of 16:1(n-7) were also those with the greatest amount of overall fatty acids (i.e., particularly lipid-rich). Generally, a strong decrease of the relative amount of PUFAs (including diatom marker FAs) from early to late bloom phase has been documented both in pelagic and sympagic environments [16,17,51,52]. While different taxonomic groups of microalgae are characterized by different fatty acid composition, our results do not support indications for taxonomically induced differences in fatty acid composition by different types of diatoms (as hypothesized in [31]).

4.3. Highly Branched Isoprenoids (HBIs)

A series of studies over the years have begun to explore the potential influence of environmental factors on the synthesis of HBIs. Until recently, these were all conducted on temperate diatom species. A seasonal influence was identified [53] by studying *Haslea ostrearia* grown outside under ambient conditions. Although the direct cause was not established, it was found that cells produced higher abundances of HBIs in early summer (6.5 pg cell^{-1}) than they did at other times of the year. The effect of salinity on *H. ostrearia* revealed the diatom to be osmotolerant [54] while yet further analysis of *H. ostrearia* growth showed some increase in cellular concentration between lag (0.3 pg cell^{-1}) and stationary phases (4.8 pg cell^{-1}) of growth [55], proving an early indication that nutrient availability might influence how cells synthesize HBIs. This idea was revisited recently to test the effect of nutrient limitation observed at the ice-water interface of sea ice where most Arctic sea ice-diatoms live [56]. Accordingly, it was confirmed that low nutrient availability can stimulate order-of-magnitude scale changes in cellular production of HBIs in the Arctic sea ice diatom *Haslea vitrea* but not in the co-inhabiting *Haslea crucigeroides* in laboratory cultures [27]. This could have a part to play in the significant differences we observed in HBI concentrations between stations. Unfortunately, however, no data exist for the response of IP$_{25}$-producing diatoms to similar environmental changes, which limits our ability to fully evaluate changes in IP$_{25}$ concentration here. That said, it is consistently evidenced that a clear distinction exists in the presence-absence of IP$_{25}$ in relation to the source organisms compared here; sea ice algae vs. phytoplankton and that this is further confirmed by our analyses.

4.4. Stable Isotope Ratios in Bulk POM and Specific Fatty Acids

A considerable variability in δ^{13}C in both sea ice algae and phytoplankton has been well documented in many studies (see, e.g., [28,30,57]), and was attributed to higher carbon uptake that had already taken place in late bloom stages compared to early bloom stages. Pineault et al. [28] documented δ^{13}C values in bottom sea ice ranging from -27.1 to -11.4‰, and found this variation related to ice protist biomass and DIC availability. These results are well in line with our findings, as the samples that were most depleted in ^{12}C stemmed from situations in which DIC reservoirs had been reduced already as a consequence of biological production. In environments that experience slow or restricted replenishment of the inorganic carbon pool, δ^{13}C-POC values become depleted in ^{12}C, e.g., during periods of rapid phytoplankton growth [58] or in dense assemblages of sea ice algae within a spatially limited habitat as a result of high sympagic primary production [7,31,59]. Previous studies documented that sympagic POM becomes enriched in ^{13}C when biomass concentrations increased [60,61]. A rapid decrease in DIC concentrations was observed at MS station during the last two weeks of April, concomitantly with the peak sea ice algal biomass development. A similar decrease in bottom-ice DIC over the same time span was reported in the Canadian Arctic Archipelago [62]. Another important factor leading to increased depletion of ^{12}C was the decreasing nitrate concentrations. This is in agreement with other studies, which identified phytoplankton growth rate, as well as the availability of carbon, light, and nutrients to affect isotopic fractionation and the δ^{13}C-POM values. In addition to these biological factors, there are also temporal and regional differences in the δ^{13}C baseline in inorganic carbon [29] which also affect δ^{13}C in POM. Thus, even the baseline signal in sea ice might undergo a pronounced temporal variation, and thereby also contribute to the high variability in δ^{13}C-POC$_{ice}$. This highlights that caution is required when using bulk δ^{13}C values of POC$_{ice}$ and POC$_{water}$ to distinguish between open water versus ice-dependent food webs in the Arctic (Søreide et al., 2006). The separation between

sympagic and pelagic communities solely based on this signal is poor, since the variability within ice algae samples is much higher than between ice algae and open water phytoplankton. The typical "ice algae signatures" (depleted in ^{12}C) are only found under limiting conditions. The application of stable isotope ratios not from bulk material, but in specific compounds allows combining fatty acid and stable isotope marker characteristics, representing a more advanced tool in the attempt to distinguish pelagic from sympagic carbon sources [7,63]. The uniqueness of CSIA is to separate fatty acids of a specific class of algae, e.g., 16:1(n-7) for diatoms and 18:4(n-3) for flagellates and relate the isotope composition to their habitat. As in all other trophic markers, however, even compound-specific stable isotope values cannot resolve the taxonomic composition down to genus or species level. Furthermore, the stable isotope signal of single fatty acids also showed temporal and spatial variability similar to the bulk signal, in response to environmental and growth conditions as shown in this study. In the context of food web studies, it should also be noted that isotopic ratios of essential PUFAs that are not metabolically modified by consumers have the greatest potential to provide reliable information on trophic structures [64], as the isotopic signal of a fatty acid molecule is determined by the number of metabolic steps during biosynthesis.

High C:N ratios and high overall lipid concentrations (normalized to POC); Figure 2 and Table 1 indicate a very late bloom development stage at both the outermost station of the transect (VMF2), as well as the latest sampling occasion at MS (2/5), in particular under low snow conditions. This is confirmed by correspondingly low nutrient and DIC concentrations. In such situations, algae switch their metabolic activities towards storage lipid formation (reflected in high 16:1(n-7), and high total lipid normalized to POC, together with a marked decrease in %PUFAs). Furthermore, they also alter the isotopic fractionation due to decreasing DIC availability, resulting in isotopic ratios depleted in ^{12}C.

4.5. Implications for Inferring Ice Algal Bloom Characteristics from Different Trophic Markers

Apart from the remarkable variability in sea ice biomarker signatures and their dependency on environmental conditions and algal physiology, the observed "patterns" in lipid and stable isotope markers have even more severe implications for their use in characterizing and understanding algal blooms. As described in the introduction, all markers are being used for trying to distinguish between sea ice algae and phytoplankton, often attempting to establish a clearly distinguishable baseline signal for further food web analyses. Hence, they should be able to also indicate relative contributions of truly sympagic species to overall sea ice POM or reflect variations in relative abundances of diatoms. In order to illustrate how the here documented variability on small temporal and spatial scales impairs such approaches, we tried inferring bloom characteristics (i.e., relative contributions of sea ice algae vs. pelagic species, or relative contribution of diatoms to overall algal biomass), from the analyzed biochemical markers along the ice core transect. Listed below are potential conclusions that could be drawn when considering only one type of marker at a time:

- FATM: It is difficult to arrive at consistent conclusions based solely on single fatty acid trophic markers as the relative contributions of the three most widely used diatom marker FAs changed strongly, with partly contrasting patterns. Highest diatom contributions were indicated by 16:1(n-7) at VMF1 and VMF2, whereas typical diatom PUFAs (16:4(n-1) and 20:5(n-3)) were highest at the shallower stations. Summarizing total diatom FAs normalized to POC yielded similar values for IS, IM, and VMF1 (appx. 0.012), with MS being lower (0.005) and VMF2 much higher (0.039). Inferences based on individual %fatty acids only are inconclusive, total diatom FAs normalized to POC indicate highest diatom contributions at VMF2, and lowest at MS.

- δ^{13}C POM: at stations VMF1 and VMF2 depleted ratios (−19 to −18‰) were reported that are typically considered to be indicative for sea ice algae, whereas MS and IM exhibited δ^{13}C values that are normally considered to be of pelagic origin (−23 to −22‰). Based on these results, we would assume highest relative contributions of sea ice algae at VMF1 and VMF2, and more "pelagic" influenced species composition in bottom sea ice at the shallower stations.

- $\delta^{13}C$ of single FAs: Isotope ratios of single fatty acids varied similar to those of bulk POM, with the exception of VMF1 that in terms of $\delta^{13}C$ 16:4(n-1) was not significantly different from MS, IM and IS, while in all other FAs, the isotopic signal at this station was between that of VMF2 and the remaining shallower stations. Based on these results, we would assume highest relative contributions of sea ice algae at VMF1 and VMF2, and more "pelagic" influenced species at the shallower stations.

- IP_{25}: the highest concentration of this ice algal biomarker (both in absolute terms, and normalized to POC) was clearly found at the shallowest stations, and—despite some variability—at MS. Almost no IP_{25} could be detected at VMF1 and VMF2, which indicates the absence (or extremely low abundances) of IP_{25} producing sea ice algae. Based on these findings, one would conclude that no sea ice diatoms (or, more specifically, IP_{25} producers) were present at VMF1 and VMF2, whereas IS and MS clearly had sea ice diatom assemblages.

It is worth noticing that these conclusions are not only variable, but partly even contradict each other (see, e.g., isotopic biomarkers vs. IP_{25}). None of the marker compounds correctly reflected the results of microscopic analyses of species composition that indicated surprisingly little variability between all transect stations, with sympagic diatoms accounting for the vast majority of biomass (around 72–84%) at all stations. However, it has to be noted that no species composition data are available for VMF2. Of the stations analyzed, VMF1 exhibited the lowest relative contribution of sympagic diatoms, which is in line with the inferences from the IP_{25}-based analyses, but contrary to the $\delta^{13}C$-based indicators. These findings illustrate the need for contextual knowledge and ancillary data (such as, e.g., nutrient or DIC concentrations and irradiance) to correctly interpret trophic marker values. Reviewing the results in light of the physiological context of bloom development also helps to arrive at a more accurate and comprehensive understanding.

4.6. Comparing Trophic Markers' Potential to Distinguish Reliably between Sea Ice Algae and Phytoplankton

Samples from a co-occurring phytoplankton bloom (also dominated by Bacillariophyceae) were taken in order to test the different markers' potentials to unambiguously distinguish between algal materials originating from sea ice vs. water samples. The fatty acid composition-based multivariate analysis showed a substantial overlap between sympagic and pelagic samples, with relatively higher values of PUFAs in sea ice samples. It is, however, important to realize that this separation is not universally valid, but highly specific for the dataset presented in the current study. To illustrate this, we applied the same analysis on another seasonal fatty acid composition dataset of sea ice algae and phytoplankton collected in Rijpfjorden (Svalbard) 2007 (Figure 10, based on [16] and unpublished phytoplankton data). Here, the distinction between samples from both habitats appears clearer. It is important to note, however, that in this case the separation between the sympagic and pelagic samples was not driven by generally higher PUFA percentages in the sea ice samples. Instead, the pelagic bloom was dominated by flagellates rather than diatoms, which was reflected in a correspondingly distinct fatty acid composition with high flagellate marker PUFAs, such as 22:6(n-3) and 18:4(n-3) (Figure 10). In the Rijpfjorden dataset, the overall relative percentage of PUFAs in sea ice algae and phytoplankton was not significantly different but varied strongly seasonally in both. The longer seasonal sampling period (April–October) for phytoplankton fatty acid composition causes the relatively greater variability in this part of the dataset. Unfortunately, HBIs and stable isotope ratios were not included in that study. In conclusion, there are no universal features of microalgal fatty acid composition that allow an unambiguous distinction of their origin with respect to habitat (sea ice vs. open water). Depending on the specific circumstances (timing of sampling relative to bloom developmental stage, taxonomic composition) samples might differ from each other, but the seasonal dynamics of algal bloom development both with respect to species succession and physiological state represents a major source of uncertainty and impairs generalizations.
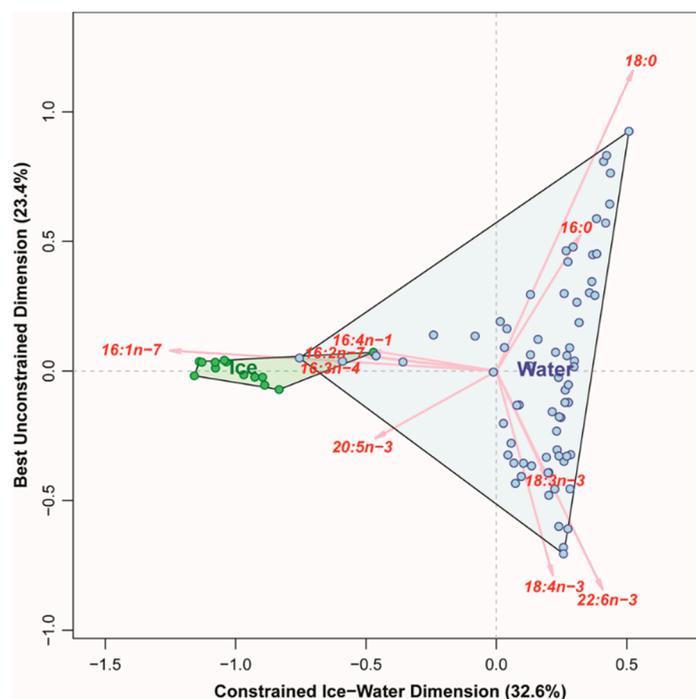
Figure 10. Distinguishing pelagic and sympagic POM samples based on their fatty acid composition, using CCA: Example from Rijpfjorden 2007 (CLEOPATRA project, [16] and unpublished data). Green dots indicate samples taken from 0–3 cm ice cores (April–June), blue from water column (March–October).

In the current study (Van Mijenfjorden 2017), the most distinct separation of sympagic and pelagic POM was achieved based on their HBI composition. Our data confirm these molecules have a much higher source-specificity than either FAs or stable isotope ratios and warrant a more robust identification of the source habitat than the other two (despite indications for environmental impacts on the amount of HBIs produced in a given algae). It is, however, important to keep in mind that IP_{25} is not produced by the most dominant species. Hence, its absence does not necessarily indicate the complete absence of sympagic algae per se, but rather the absence of IP_{25} producers in particular.

$\delta^{13}C$ values of both bulk POC and single marker fatty acids proved to be variable and displayed values "typical" for sympagic algae (i.e., enriched in ^{13}C), only under conditions where nitrate was limiting, and DIC concentrations indicated a well-advanced bloom development. This is in line with previous findings [28,30,31], with the only difference being that these authors attributed the increase in $\delta^{13}C$ of diatom FA markers to increased light availability. Due to the strong correlation of light and nutrient availability in the field, and the co-regulation of primary production by both factors, it is impossible to clearly separate the respective influence of any of them without experimental studies with a factorial design. However, increased light availability (i.e., season progression), as well as decreased nutrient availability, are also both indicative of a rather advanced stage of bloom development with substantial production having taken place, and correspondingly limiting conditions prevailing. The major characteristics, advantages and pitfalls of all analyzed trophic markers are shortly summarized in Table 3.

<div align="center">**Table 3.** Trophic marker characteristics summarized.</div>

	Unambiguously Specific for Sea Ice Algae vs. Phytoplankton	Produced in Dominating Species	Reflects Species Composition	Changes with Growth Conditions	Distinction between Sympagic and Pelagic POM Based on
HBIs	Yes	No	+/− HBI producer	? (probably yes)	Specific compounds, exclusively produced by some species belonging to only one of the groups
FATM	No	Yes	yes (group level)	Relative composition changes	Not possible—unless major taxonomic differences between both groups
δ^{13}C POC	Sometimes	Yes	No	Yes	Higher δ^{13}C (average from bulk POC) in sympagic communities due to high biomass densities and slow replenishment of DIC pool in spatially restricted environments only found under limited conditions
δ^{13}C FATM	Sometimes	Yes	No	Yes	Higher δ^{13}C (in a single compound) in sympagic communities due to high biomass densities and slow replenishment of DIC pool in spatially restricted environment—only found under limited conditions

5. Conclusions

The application of lipid- or stable isotope-based trophic markers for food web analyses is a valuable tool in trophic ecology but has to be carried out with some caution. Ancillary data elucidating the overall context of the sampling situation (pre-, peak-, or post-bloom) are key to correctly interpret and use biochemical signals in algal communities. A rough estimate of the method-intrinsic error caused by natural variability of the baseline signal is essential and should be taken into consideration when extrapolating the results of food-web analyses towards higher-level conclusions. None of the presented trophic markers are capable of distinguishing between sympagic and pelagic sources on their own, but their combined use increases the robustness of results with significant implications on any conclusions drawn from them. Therefore, we recommend that in future studies, as many of these as possible should be combined and assessed within the context of detailed environmental data to limit misinterpretation of field data.

Author Contributions: E.L. conceptualized the study and drafted the manuscript; E.L., T.A.B., S.V., A.C.K. and J.W. contributed in the collection of field data; T.A.B. and M.G. analyzed lipid biomarkers in algal material; J.W. performed the taxonomic analyses and biomass calculations; C.J.M.H. led nutrient sample analyses; A.C.K. analyzed samples for Chl a; A.F. and M.C. analyzed DIC concentrations and calculated carbon drawdown;

References

1. Arrigo, K.R.; van Dijken, G.; Pabi, S. Impact of a shrinking Arctic ice cover on marine primary production. *Geophys. Res. Lett.* **2008**, *35*. [CrossRef]

2. Huntington, H.P.; Danielson, S.L.; Wiese, F.K.; Baker, M.; Boveng, P.; Citta, J.J.; Robertis, A.D.; Dickson, D.M.S.; Farley, E.; George, J.C.; et al. Evidence suggests potential transformation of the Pacific Arctic ecosystem is underway. *Nat. Clim. Chang.* **2020**, *10*, 342–348. [CrossRef]

3. Grebmeier, J.M.; Overland, J.E.; Moore, S.E.; Farley, E.V.; Carmack, E.C.; Cooper, L.W.; Frey, K.E.; Helle, J.H.; McLaughlin, F.A.; McNutt, S.L. A major ecosystem shift in the northern Bering Sea. *Science* **2006**, *311*, 1461–1464. [CrossRef] [PubMed]

4. Soreide, J.E.; Falk-Petersen, S.; Hegseth, E.N.; Hop, H.; Carroll, M.L.; Hobson, K.A.; Blachowiak-Samolyk, K. Seasonal feeding strategies of Calanus in the high-Arctic Svalbard region. *Deep Sea Res. Part II-Top. Stud. Oceanogr.* **2008**, *55*, 2225–2244. [CrossRef]

5. Brown, T.A.; Belt, S.T.; Piepenburg, D. Evidence for a pan-Arctic sea-ice diatom diet in *Strongylocentrotus* spp. *Polar Biol.* **2012**, *35*, 1281–1287. [CrossRef]

6. Brown, T.A.; Galicia, M.P.; Thiemann, G.W.; Belt, S.T.; Yurkowski, D.J.; Dyck, M.G. High contributions of sea ice derived carbon in polar bear (*Ursus maritimus*) tissue. *PLoS ONE* **2018**, *13*. [CrossRef]

7. Budge, S.M.; Wooller, M.J.; Springer, A.M.; Iverson, S.J.; McRoy, C.P.; Divoky, G.J. Tracing carbon flow in an arctic marine food web using fatty acid-stable isotope analysis. *Oecologia* **2008**, *157*, 117–129. [CrossRef]

8. Søreide, J.E.; Hop, H.; Carroll, M.; Falk-Petersen, S.; Hegseth, E.N. Seasonal food web structures and sympagic-pelagic coupling in the European Arctic revealed by stable isotopes and a two-source food web model. *Prog. Oceanogr.* **2006**, *71*, 59–87. [CrossRef]

9. Kohlbach, D.; Ferguson, S.H.; Brown, T.A.; Michel, C. Landfast sea ice-benthic coupling during spring and potential impacts of system changes on food web dynamics in Eclipse Sound, Canadian Arctic. *Mar. Ecol. Prog. Ser.* **2019**, *627*, 33–48. [CrossRef]

10. Tamelander, T.; Renaud, P.E.; Hop, H.; Carroll, M.L.; Ambrose, W.G.; Hobson, K.A. Trophic relationships and pelagic-benthic coupling during summer in the Barents Sea Marginal Ice Zone, revealed by stable carbon and nitrogen isotope measurements. *Mar. Ecol. Prog. Ser.* **2006**, *310*, 33–46. [CrossRef]

11. Jónasdóttir, S.H. Fatty acid profiles and production in marine phytoplankton. *Mar. Drugs* **2019**, *17*, 151. [CrossRef] [PubMed]

12. Dalsgaard, J.; St John, M.; Kattner, G.; Muller-Navarra, D.; Hagen, W. Fatty acid trophic markers in the pelagic marine environment. *Adv. Mar. Biol.* **2003**, *46*, 225–340. [PubMed]

13. Reitan, K.I.; Rainuzzo, J.R.; Olsen, Y. Effect of nutrient limitation on fatty acid and lipid content of marine microalgae. *J. Phycol.* **1994**, *30*, 972–979. [CrossRef]

14. Thompson, P.A.; Guo, M.; Harrison, P.J. The influence of irradiance on the biochemical composition of 3 phytoplankton species and their nutritional value for larvae of the pacific oyster (*Crassostrea gigas*). *Mar. Biol.* **1993**, *117*, 259–268. [CrossRef]

15. Thompson, P.A.; Guo, M.X.; Harrison, P.J.; Whyte, J.N.C. Effects of variation in temperature on the fatty acid composition of 8 species of marine phytoplankton. *J. Phycol.* **1992**, *28*, 488–497. [CrossRef]

16. Leu, E.; Wiktor, J.; Soreide, J.; Berge, J.; Falk-Petersen, S. Increased irradiance reduces food quality of sea ice algae. *Mar. Ecol. Prog. Ser.* **2010**, *411*, 49–60. [CrossRef]

17. Leu, E.; Falk-Petersen, S.; Kwaśniewski, S.; Wulff, A.; Edvardsen, K.; Hessen, D.O. Fatty acid dynamics during the spring bloom in a High Arctic fjord: Importance of abiotic factors versus community changes. *Can. J. Fish. Aquat. Sci.* **2006**, *63*, 2760–2779. [CrossRef]

18. Leu, E.; Wängberg, S.-Å.; Wulff, A.; Falk-Petersen, S.; Borre Orbaek, J.; Hessen, D.O. Effects of changes in ambient PAR and UV radiation on the nutritional quality of an Arctic diatom (*Thalassiosira antarctica var. borealis*). *J. Exp. Mar. Biol. Ecol.* **2006**, *337*, 65–81. [CrossRef]

19. Brown, T.A.; Belt, S.T.; Tatarek, A.; Mundy, C.J. Source identification of the Arctic sea ice proxy IP25. *Nat. Commun.* **2014**, *5*. [CrossRef]

20. Belt, S.T.; Masse, G.; Rowland, S.J.; Poulin, M.; Michel, C.; LeBlanc, B. A novel chemical fossil of palaeo sea ice: IP25. *Organ. Geochem.* **2007**, *38*, 16–27. [CrossRef]

21. Volkman, J.K.; Barrett, S.M.; Dunstan, G.A. C25 and C30 highly branched isoprenoid alkenes in laboratory cultures of two marine diatoms. *Organ. Geochem.* **1994**, *21*, 407–413. [CrossRef]

22. Limoges, A.; Massé, G.; Weckström, K.; Poulin, M.; Ellegaard, M.; Heikkilä, M.; Geilfus, N.-X.; Sejr, M.K.; Rysgaard, S.; Ribeiro, S. Spring succession and vertical export of diatoms and IP25 in a seasonally ice-covered high Arctic Fjord. *Front. Earth Sci.* **2018**, *6*. [CrossRef]

23. Amiraux, R.; Smik, L.; Köseoğlu, D.; Rontani, J.-F.; Galindo, V.; Grondin, P.-L.; Babin, M.; Belt, S.T. Temporal evolution of IP$_{25}$ and other highly branched isoprenoid lipids in sea ice and the underlying water column during an Arctic melting season. *Elem. Sci. Anth.* **2019**, *7*, 38. [CrossRef]

24. Brown, T.A.; Belt, S.T.; Philippe, B.; Mundy, C.J.; Masse, G.; Poulin, M.; Gosselin, M. Temporal and vertical variations of lipid biomarkers during a bottom ice diatom bloom in the Canadian Beaufort Sea: Further evidence for the use of the IP25 biomarker as a proxy for spring Arctic sea ice. *Polar Biol.* **2011**, *34*, 1857–1868. [CrossRef]

25. Brown, T.A.; Belt, S.T. Biomarker-based H-Print quantifies the composition of mixed sympagic and pelagic algae consumed by *Artemia* sp. *J. Exp. Mar. Biol. Ecol.* **2017**, *488*, 32–37. [CrossRef]

26. Brown, T.A.; Yurkowski, D.J.; Ferguson, S.H.; Alexander, C.; Belt, S.T. H-Print: A new chemical fingerprinting approach for distinguishing primary production sources in Arctic ecosystems. *Environ. Chem. Lett.* **2014**, *12*, 387–392. [CrossRef]

27. Brown, T.A.; Rad-Menéndez, C.; Ray, J.L.; Skaar, K.S.; Thomas, N.; Ruiz-Gonzalez, C.; Leu, E. Influence of nutrient availability on Arctic sea ice diatom HBI lipid synthesis. *Organ. Geochem.* **2020**, *141*, 103977. [CrossRef]

28. Pineault, S.; Tremblay, J.-E.; Gosselin, M.; Thomas, H.; Shadwick, E. The isotopic signature of particulate organic C and N in bottom ice: Key influencing factors and applications for tracing the fate of ice-algae in the Arctic Ocean. *J. Geophys. Res. Oceans* **2013**, *118*, 287–300. [CrossRef]

29. de la Vega, C.; Jeffreys, R.M.; Tuerena, R.; Ganeshram, R.; Mahaffey, C. Temporal and spatial trends in marine carbon isotopes in the Arctic Ocean and implications for food web studies. *Glob. Chang. Biol.* **2019**, *25*, 4116–4130. [CrossRef]

30. Tamelander, T.; Kivimäe, C.; Bellerby, R.G.J.; Renaud, P.E.; Kristiansen, S. Base-line variations in stable isotope values in an Arctic marine ecosystem: Effects of carbon and nitrogen uptake by phytoplankton. *Hydrobiologia* **2009**, *630*, 63–73. [CrossRef]

31. Wang, S.W.; Budge, S.M.; Gradinger, R.R.; Iken, K.; Wooller, M.J. Fatty acid and stable isotope characteristics of sea ice and pelagic particulate organic matter in the Bering Sea: Tools for estimating sea ice algal contribution to Arctic food web production. *Oecologia* **2014**, *174*, 699–712. [CrossRef]

32. Hoyland, K.V. Ice thickness, growth and salinity in Van Mijenfjorden, Svalbard, Norway. *Polar Res.* **2009**, *28*, 339–352. [CrossRef]

33. Osuch, M.; Wawrzyniak, T. Inter- and intra-annual changes in air temperature and precipitation in western Spitsbergen. *Int. J. Climatol.* **2017**, *37*, 3082–3097. [CrossRef]

34. Gosselin, M.; Legendre, L.; Therriault, J.C.; Demers, S.; Rochet, M. Physical control of the horizontal patchiness of sea-ice microalgae. *Mar. Ecol. Prog. Ser.* **1986**, *29*, 289–298. [CrossRef]

35. Garrison, D.L.; Buck, K.R. Organism losses during ice melting: A serious bias in sea ice community studies. *Polar Biol.* **1986**, *6*, 237–239. [CrossRef]

36. Brown, T.A. Stability of the lipid biomarker H-Print within preserved animals. *Polar Biol.* **2018**, *41*, 1901–1905. [CrossRef]

37. Boissonnot, L.; Niehoff, B.; Hagen, W.; Søreide, J.E.; Graeve, M. Lipid turnover reflects life-cycle strategies of small-sized Arctic copepods. *J. Plankton Res.* **2016**. [CrossRef]

38. Utermöhl, H. Zur Vervollkommnung der quantitativen Phytoplankton Methodik. *Mitt. Int. Ver. Limnol.* **1958**, *9*, 1–38. [CrossRef]

39. Olenina, I. Biovolumes and Size-Classes of Phytoplankton in the Baltic Sea. Available online: https://epic.awi.de/id/eprint/30141/ (accessed on 21 June 2020).

40. Dickson, A.G.; Sabine, C.L.; Christian, J.R.; Bargeron, C.P. North Pacific Marine Science Organization. In *Guide to Best Practices for Ocean CO$_2$ Measurements*; Dickson, A.G., Sabine, C.L., Christian, J.R., Bargeron, C.P., North Pacific Marine Science Organization, Eds.; North Pacific Marine Science Organization: Sidney, BC, Australia, 2007; ISBN 978-1-897176-07-8.

41. Higgins, J.J. *Introduction to Modern Nonparametric Statistics*; Duxbury Advanced Series: Pacific Grove, CA, USA, 2004; ISBN 0-534-38775-6.

42. Benjamini, Y.; Hochberg, Y. Controlling the false discovery rate: A practical and powerful approach to multiple testing. *J. R. Stat. Soc. Ser. B Method* **1995**, *57*, 289–300. [CrossRef]

43. Greenacre, M. Data reporting and visualization in ecology. *Polar Biol.* **2016**, *39*, 2189–2205. [CrossRef]

44. Kvernvik, A.C.; Hoppe, C.J.M.; Greenacre, M.; Verbiest, S.; Wiktor, J.; Gabrielsen, T.M.; Reigstad, M.; Leu, E. Arctic sea ice algae differ markedly from phytoplankton in their ecophysiological characteristics. *Mar. Ecol. Progress Ser.* in press.

45. Leu, E.; Graeve, M.; Wulff, A. A (too) bright future? Arctic diatoms under radiation stress. *Polar Biol.* **2016**, *39*, 1711–1724. [CrossRef]

46. Kvernvik, A.C.; Rokitta, S.D.; Leu, E.; Harms, L.; Gabrielsen, T.M.; Rost, B.; Hoppe, C.J.M. Higher sensitivity towards light stress and ocean acidification in an Arctic sea-ice-associated diatom compared to a pelagic diatom. *New Phytol.* **2020**, *226*, 1708–1724. [CrossRef]

47. Cosgrove, J.P.; Church, D.F.; Pryor, W.A. The kinetics of the autoxidation of polyunsaturated fatty acids. *Lipids* **1987**, *22*, 299–304. [CrossRef] [PubMed]

48. Girotti, A.W. Photosensitized oxidation of membrane lipids: Reaction pathways, cytotoxic effects, and cytoprotective mechanisms. *J. Photochem. Photobiol. B Biol.* **2001**, *63*, 103–113. [CrossRef]

49. Mayzaud, P.; Claustre, H.; Augier, P. Effect of variable nutrient supply on fatty acid composition of phytoplankton grown in an enclosed experimental ecosystem. *Mar. Ecol. Prog. Ser.* **1990**, *60*, 123–140. [CrossRef]

50. Hayakawa, K.; Handa, N.; Kawanobe, K.; Wong, C.S. Factors controlling the temporal variation of fatty acids in particulate matter during a phytoplankton bloom in a marine mesocosm. *Mar. Chem.* **1996**, *52*, 233–244. [CrossRef]

51. Skerratt, J.H.; Nichols, P.D.; McMeekin, T.A.; Burton, H. Seasonal and inter-annual changes in planktonic biomass and community structure in eastern Antarctica using signature lipids. *Mar. Chem.* **1995**, *51*, 93–113. [CrossRef]

52. Mayzaud, P.; Chanut, J.P.; Ackman, R.G. Seasonal changes of the biochemical composition of marine particulate matter with special reference to fatty acids and sterols. *Mar. Ecol. Prog. Ser.* **1989**, *56*, 189–204. [CrossRef]

53. Wraige, J.E.; Belt, T.S.; Lewis, A.C.; Cooke, A.D.; Robert, J.-M.; Massé, G.; Rowland, S.J. Variations in structures and distributions of C25 highly branched isoprenoid (HBI) alkenes in cultures of the diatom, Haslea ostrearia (Simonsen). *Organ. Geochem.* **1997**, *27*, 497–505. [CrossRef]

54. Wraige, E.J.; Belt, S.T.; Massé, G.; Robert, J.-M.; Rowland, S.J. Variations in distributions of C25 highly branched isoprenoid (HBI) alkenes in the diatom, Haslea ostrearia: Influence of salinity. *Organ. Geochem.* **1998**, *28*, 855–859. [CrossRef]

55. Wraige, E.J.; Johns, L.; Belt, S.T.; Massé, G.; Robert, J.-M.; Rowland, S. Highly branched C25 isoprenoids in axenic cultures ofHaslea ostrearia. *Phytochemistry* **1999**, *51*, 69–73. [CrossRef]

56. Dieckmann, G.; Hellmer, H. The Importance of Sea Ice: An Overview. Available online: https://epic.awi.de/id/eprint/21259/ (accessed on 17 June 2020).

57. Gradinger, R.R.; Kaufman, M.R.; Bluhm, B.A. Pivotal role of sea ice sediments in the seasonal development of near-shore Arctic fast ice biota. *Mar. Ecol. Progress Ser.* **2009**, *394*, 49–63. [CrossRef]

58. Rau, G.H.; Takahashi, T.; Des Marais, D.J.; Repeta, D.J.; Martin, J.H. The relationship between δ^{13}C of organic matter and (CO_2 (aq)) in ocean surface water: Data from a JGOFS site in the northeast Atlantic Ocean and a model. *Geochim. Cosmochim. Acta* **1992**, *56*, 1413–1419. [CrossRef]

59. Søreide, J.E.; Carroll, M.L.; Hop, H.; Ambrose, W.G., Jr.; Hegseth, E.N.; Falk-Petersen, S. Sympagic-pelagic-benthic coupling in Arctic and Atlantic waters around Svalbard revealed by stable isotopic and fatty acid tracers. *Mar. Biol. Res.* **2013**, *9*, 831–850. [CrossRef]

60. Tremblay, J.E.; Michel, C.; Hobson, K.A.; Gosselin, M.; Price, N.M. Bloom dynamics in early opening waters of the Arctic Ocean. *Limnol. Oceanogr.* **2006**, *51*, 900–912. [CrossRef]

61. Gradinger, R. Sea-ice algae: Major contributors to primary production and algal biomass in the Chukchi and Beaufort Seas during May/June 2002. *Deep Sea Res. Part II Top. Stud. Oceanogr.* **2009**, *56*, 1201–1212. [CrossRef]

62. Fransson, A.; Chierici, M.; Miller, L.A.; Carnat, G.; Shadwick, E.; Thomas, H.; Pineault, S.; Papakyriakou, T.N. Impact of sea-ice processes on the carbonate system and ocean acidification at the ice-water interface of the Amundsen Gulf, Arctic Ocean. *J. Geophys. Res. Oceans* **2013**, *118*, 7001–7023. [CrossRef]

63. Wang, S.W.; Budge, S.M.; Iken, K.; Gradinger, R.R.; Springer, A.M.; Wooller, M.J. Importance of sympagic production to Bering Sea zooplankton as revealed from fatty acid-carbon stable isotope analyses. *Mar. Ecol. Progress Ser.* **2015**, *518*, 31–50. [CrossRef]

64. Burian, A.; Nielsen, J.M.; Hansen, T.; Bermudez, R.; Winder, M. The potential of fatty acid isotopes to trace trophic transfer in aquatic food-webs. *Philos. Trans. R. Soc. B Biol. Sci.* **2020**, *375*, 20190652. [CrossRef]